Photo-Ionization Cross Section of Beryllium near Threshold*

P. L. ALTICK
Physics Department, University of Nevada, Reno, Nevada 89507
(Received 20 November 1967)

The ^1P continuum wave functions of beryllium with energies from 0 to ~3.5 eV above the $2s$ threshold are calculated with the inclusion of auto-ionizing lines by configuration interaction. These functions are then combined with a ten-configuration ground-state function to compute the photo-ionization cross section which is found to be dominated by auto-ionization from the $2pns$ and the $2pnd$ series. The energy region studied contains the first three $2pns$ lines, which have widths of a significant fraction of a volt, comparable to their separation; and the first two $2pnd$ lines, which are about a thousand times narrower. There are no experimental measurements of the cross section for comparison; however, the computed phase shift agrees reasonably well with recent close-coupling calculations.

I. INTRODUCTION

THERE has been considerable investigation lately, both theoretical and experimental, of resonances that occur in the electron-scattering or photo-ionization cross sections of atomic systems.[1] In application to helium, it has previously been shown that the location and shape of these resonances or auto-ionization lines can be found using the method of configuration interaction in the continuum,[2] as well as the close-coupling approach.[3]

In this paper, a calculation of the photo-ionization cross section of beryllium from the $2s$ threshold to ~3.5 eV above threshold is made using configuration interaction. In this region are five auto-ionizing levels arising from $2pns$ and $2pnd$ configurations which are analyzed. The general procedure is the same as was followed for helium in I.

The nature of the results, however, is quite different from helium where the resonances are narrow and isolated, and contribute a negligible amount of oscillator strength to the background continuum. In beryllium, the auto-ionizing series and the continuum both arise from the $n=2$ shell resulting in strong coupling (broad lines) for the $2pns$ series; also the oscillator strength of this series predominates over the weak strength of the continuum. These two effects form a cross section which is completely dominated by auto-ionization and in which the lines are so broad that the cross section loses the appearance of lines superimposed upon a background. In fact, though, auto-ionization is known to dominate the near-threshold cross section for other alkaline earths through measurements on calcium by Ditchburn and Hudson,[4] strontium by Garton *et al.*,[5] and barium by Garton and Codling.[6]

Though there are no measurements on beryllium, it was selected for study as the simplest of the alkaline earths and also as a natural extension of the helium work in that, in the core approximation (which is expected to be very good here), the problem is formulated as a two-electron calculation with one continuum and two auto-ionizing series.

In the following three sections, the theory, the numerical techniques, and the calculational results are presented. The results include the photo-ionization cross section from 0 to ~3.5 eV above threshold, the ^1P phase shift in the same region, and the locations of the five lowest ^1P and ^3P resonances calculated with a discrete matrix.

II. THEORY

In this section, the equations which are used to find the excited-state functions and the expression for the cross section are presented. The excited states of interest are all ^1P in Russell-Saunders coupling and, to be definite, the projection quantum number M is chosen equal to zero. Since all the states have the same symmetry, it will not be specifically noted.

The configurations to be included are conveniently classified into three categories—bound, continuum, and auto-ionizing. For the region of the spectrum considered here, there is just one continuum, $1s^22s\epsilon p$. (From here on the $1s^2$ notation will be dropped, since, in the core approximation, this shell is occupied in all configurations.) The continuum and bound configurations, designated ψ_ϵ and ψ_i, respectively, represent the $2s$ continuum and the $2s$ Rydberg series. In the above, the notation i or ϵ denotes all quantum numbers necessary to specify a particular configuration. The auto-ionizing configurations, designated χ_i, are configurations in which both electrons are in bound orbitals but which lie energetically above the $2s$ threshold. Two series of auto-ionizing levels are included: $2pns$ and $2pnd$, where $n \geqslant 3$.

* This research was supported in part by the National Aeronautics and Space Administration under Grant No. NGR-29-001-008.

[1] A review of the subject along with earlier references may be found in the article by P. G. Burke, Advan. Phys. **14**, 521 (1965).

[2] P. L. Altick and E. N. Moore, Phys. Rev. **147**, 59 (1966), hereafter called I.

[3] P. G. Burke and D. D. McVicar, Proc. Phys. Soc. (London) **86**, 989 (1965).

[4] R. W. Ditchburn and R. D. Hudson, Proc. Roy. Soc. (London) **A256**, 53 (1960).

[5] W. R. S. Garton, K. Codling, W. M. Parkinson, E. M. Reeves, and G. L. Grasdalen, Harvard College Observatory Scientific Report No. 21, 1967 (unpublished).

[6] W. R. S. Garton and K. Codling, Proc. Phys. Soc. (London) **75**, 87 (1960).

The Hartree-Fock basis set chosen for this calculation yields a diagonal matrix in the $2s$ channel. This point will be discussed in more detail in the next section, but accepting it for now, the only nonzero interaction matrix elements couple the $2s$ and $2p$ channels or, to put it another way, couple auto-ionizing configurations with the bound and continuum configurations. Thus the matrix elements are denoted as follows:

$$\begin{aligned}
&(\psi_i|H|\psi_j)=\delta_{ij}e_i,\\
&(\psi_i|H|\psi_\epsilon)=0,\\
&(\psi_i|H|\chi_j)=V_{ij},\\
&(\psi_\epsilon|H|\psi_{\epsilon'})=\delta(\epsilon-\epsilon')\epsilon,\\
&(\psi_\epsilon|H|\chi_j)=V_{\epsilon j},\\
&(\chi_i|H|\chi_j)=U_{ij},
\end{aligned} \tag{1}$$

where H is the Coulomb Hamiltonian for the beryllium atom.

The excited-state wave function, for energy E, is expanded as

$$\Psi_E=\sum_i a_i\psi_i+\sum_i f_i\chi_i+\int d\epsilon' a_{\epsilon'}\psi_{\epsilon'}. \tag{2}$$

The coefficients a_i, f_i, and a_ϵ also depend on E, but for simplicity of notation, this dependence is not explicitly shown. The equations for the coefficients are then

$$(E-e_i)a_i-\sum_j V_{ij}f_j=0, \tag{3a}$$

$$(E-U_{ii})f_i-\sum_{j\neq i}U_{ij}f_j-\sum_j V_{ij}a_j-\int d\epsilon' V_{\epsilon' i}a_{\epsilon'}=0, \tag{3b}$$

$$(E-\epsilon)a_\epsilon-\sum_j V_{\epsilon j}f_j=0. \tag{3c}$$

The singularity in a_ϵ is treated by introducing a smoothly varying coefficient b_ϵ, where

$$a_\epsilon=P[b_\epsilon/(E-\epsilon)]+\beta(E)b_E\delta(E-\epsilon). \tag{4}$$

With Eq. (4), Eqs. (3b) and (3c) become

$$(E-U_{ii})f_i-\sum_{j\neq i}U_{ij}f_j-\sum_j V_{ij}a_j-P\int d\epsilon'\frac{V_{\epsilon' i}b_{\epsilon'}}{E-\epsilon'}-\beta(E)b_E V_{iE}=0, \tag{5a}$$

$$b_\epsilon-\sum_j V_{\epsilon j}f_j=0. \tag{5b}$$

To reduce the size of the final matrix and to include implicitly the infinite number of bound configurations, the a_i amplitudes are eliminated by using Eq. (3a). This substitution alters Eqs. (5) to read

$$(E-U_{ii}')f_i-\sum_{j\neq i}U_{ij}'f_j-P\int d\epsilon'\frac{V_{\epsilon' i}b_{\epsilon'}}{E-\epsilon'}-\beta(E)b_E V_{iE}=0, \tag{6a}$$

$$b_\epsilon-\sum_j V_{\epsilon j}f_j=0, \tag{6b}$$

where

$$U_{ij}'=U_{ij}+\sum_l\frac{V_{li}V_{lj}}{(E-e_l)} \tag{7}$$

is a matrix element modified by the Rydberg series of states ψ_l. The sum over l includes the entire series, and its evaluation is discussed in Sec. III. Equations (6) are now in a form amenable to numerical solution which was carried out for various energies yielding excited-state wave functions Ψ_E, and also the phase shift $\delta(E)$, with respect to the basis, given by

$$\delta(E)=-\tan^{-1}[\pi/\beta(E)]. \tag{8}$$

The ground-state wave function Ψ_G needed to compute the cross section was also found by configuration interaction in the usual manner. A description of this function is given in Sec. III.

With Ψ_G and Ψ_E known, the cross section, in the dipole length formulation, follows by evaluating

$$(\Psi_G|Z|\Psi_E)=\sum_j(\Psi_G|Z|\chi_j)f_j+\sum_j(\Psi_G|Z|\psi_j)a_j+P\int d\epsilon'\frac{(\Psi_G|Z|\psi_{\epsilon'})}{(E-\epsilon')}b_{\epsilon'}+\beta(E)b_E(\Psi_G|Z|\psi_E), \tag{9}$$

where Z is the z component of the total dipole operator for the atom. Again eliminating the amplitudes a_j leads to

$$(\Psi_G|Z|\Psi_E)=\sum_j(\Psi_G|Z|X_j)f_j+P\int d\epsilon'\frac{(\Psi_G|Z|\psi_{\epsilon'})}{(E-\epsilon')}b_{\epsilon'}+\beta(E)b_E(\Psi_G|Z|\psi_E), \tag{10}$$

where

$$(\Psi_G|Z|X_i)=(\Psi_G|Z|\chi_i)+\sum_l\frac{V_{li}(\Psi_G|Z|\psi_l)}{(E-e_l)} \tag{11}$$

is a dipole element modified by the Rydberg series. The expression for the cross section in Mb (10^{-18} cm^2) with the excitation energy ΔE in a.u. is

$$\sigma(E)=8.067\Delta E|(\Psi_G|Z|\Psi_E)|^2. \tag{12}$$

The physical constants in this expression were taken from Du Mond and Cohen.[7] Throughout the paper atomic units are used unless otherwise noted, and no reduced mass corrections are made.

III. NUMERICAL TECHNIQUES

The numerical work consisted of: (1) generation of the basis set; (2) computation of Coulomb and dipole matrix elements; (3) diagonalization of the energy matrix and computation of the cross section. These phases of the calculation will be discussed in turn.

The explicit configurations used for the excited-state calculation are: $2snp$, $n=2$, 9; $2skp$, $k=0$, 1.6 with a mesh of $\Delta k=0.2$; $2pns$, $n=3$, 6; and $2pnd$, $n=3$, 6. The momentum k is used here instead of the energy ϵ because the integrals over the continuum were performed with k as the variable. The kinetic energy of the free electron at a great distance from the atom is, of course, $\frac{1}{2}k^2$. The configurations used for the ground-state calculation are $2s^2$, $2s3s$, $2s4s$, $3s^2$, $4s^2$, $2p^2$, $3p^2$, $4p^2$, $3d^2$, and $4d^2$. This particular choice was taken from the work of Weiss.[8]

The orbitals composing these configurations were computed in two distinct potentials. First, the $2s$ and all other orbitals used in the auto-ionizing configurations and in the ground-state calculation were computed in the Hartree-Fock field of the $1s$ electrons only, i.e., the field of Be^{++}. Second, the p orbitals to form the bound and continuum configurations were computed in the Hartree-Fock field of the $1s$ core and the $2s$ electron such that the over-all state is a singlet. The $1s$ orbital used was taken from the Hartree-Fock calculation of the ground state of Be^{++} by Roothaan *et al.*[9] and was not varied during the calculation.

The virtues of such a basis are: (1) There is no coupling of the bound and continuum configurations among themselves resulting in far fewer matrix elements to compute. This follows from the observation that the variational principle applied to a wave function with all orbitals fixed but one yields the Hartree-Fock equation for the unspecified orbital that is solved here. (2) The orbitals used for the auto-ionizing configurations and the ground state are drawn in toward the nucleus compared to a screened set and are thus expected to provide faster convergence for the configuration interactions. This basis is still orthogonal in the two-electron space because of the orthogonality of the s orbitals, but not in a one-electron space. Thus matrix elements of one-particle operators will contain overlap integrals.

The numerical integration method used to find the Hartree-Fock orbitals is basically the same as used earlier by Altick and Glassgold and is discussed there.[10] This method was extended to include nonlocal potentials by employing, with a few modifications, the noniterative approach of Marriot.[11]

The Coulomb matrix elements needed, as well as dipole-length matrix elements and overlap integrals, were performed numerically using Simpson's rule.

The evaluation of the sums appearing in Eqs. (7) and (11) was accomplished as follows: Terms up to and including $2s9p$ were found explicitly. For the remainder of the sum, the relations

$$\frac{V_{ij}}{V_{il}}=\left(\frac{n_l-d}{n_j-d}\right)^{3/2} \tag{13a}$$

and

$$e_l=E_0-1/2(n_l-d)^2 \tag{13b}$$

were employed, where n_l is the principal quantum number of the p orbital in the lth configuration, d is the quantum defect of the series, and E_0 is the energy of the ion which is lacking the running electron. These relations are valid if n_l and n_j are much larger than the principal quantum number of any other orbital appearing in the element. Equation (13a) is also used with the dipole elements. Writing $E=E_0+\frac{1}{2}k^2$, the sum to be evaluated, lacking a constant multiplier, becomes

$$\sum_{n=10}^{\infty}\frac{1}{(n-d)^3[k^2+1/(n-d)^2]}=\sum_{n=10}^{\infty}\frac{1}{(n-d)[k^2(n-d)^2+1]}. \tag{14}$$

This expression was evaluated by explicit summing up to $n=100$ and replacing the remainder with an integral, i.e.,

$$\sum_{n=101}^{\infty}\frac{1}{(n-d)[k^2(n-d)^2+1]}\approx\int_{101-d}^{\infty}\frac{dx}{x(k^2x^2+1)}=\ln\left[\frac{1}{k^2(101-d)^2}+1\right]. \tag{15}$$

Since for all energies studied here, the integral contributes a small amount to the entire sum, and the Rydberg approximations of Eq. (13) are valid to a high degree, this procedure which allows the inclusion of all bound configurations should yield sums accurate to at least a few percent.

With the matrix elements known, the next step is the formation and diagonalization of the energy matrix. This is accomplished just as in I and need not be described further. Once the matrix is diagonalized, the finding of the cross section proceeds also as in I.

IV. RESULTS

Before presenting the results of the calculation, a resume of approximations will be made. (1) Configura-

[7] E. R. Cohen and J. W. M. Du Mond, Rev. Mod. Phys. **37**, 537 (1965).
[8] A. W. Weiss (private communication).
[9] C. C. J. Roothaan, L. M. Sachs, and A. W. Weiss, Rev. Mod. Phys. **32**, 186 (1960).
[10] P. L. Altick and A. E. Glassgold, Phys. Rev. **133**, A632 (1964).
[11] R. Marriot, Proc. Phys. Soc. (London) **72**, 121 (1958).

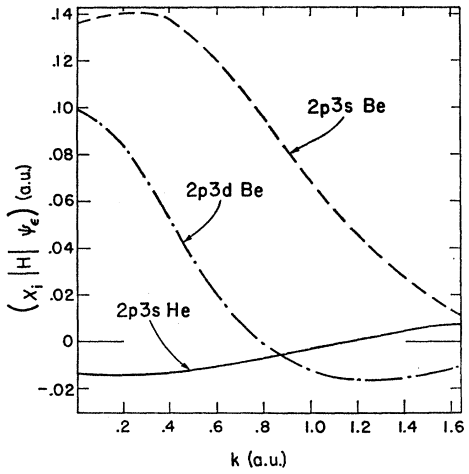

FIG. 1. A plot of some sample matrix elements coupling the continuum to the auto-ionizing states in beryllium and helium. The much greater strength of the coupling in beryllium is noteworthy.

tions involving the excitation of $1s$ electrons out of the core are neglected as the processes under study here involve energies much less than the binding energy of the $1s$ shell. The effect of this neglect was looked into by calculating some sample interaction matrix elements between core configurations and auto-ionizing configurations. It was found that coupling of the core configurations is down by two orders of magnitude from the mixing of auto-ionizing configurations among themselves. Of course, the shell structure of beryllium is particularly favorable for the core approximation and that is one reason why it was selected for study. (2) All auto-ionizing series with limits at the $n \geqslant 3$ shells were omitted. This omission is based on the fact that reasonable results were obtained without these series in the helium calculation, and the energy separation between the $n=2$ and $n=3$ shells is about the same in both cases. (3) Members of the $2pns$ and $2pnd$ series with $n>6$ were not included. This cutoff was chosen because such a truncated set gave positions of ^3P auto-ionizing levels which agreed well with experimental data (to be described later), and also because a similar cutoff in helium led to satisfactory results. However, in the next section, a demonstration of the effect of this truncation on the phase shift will be given. (4) The continuum was cut off at $\frac{1}{2}k^2=1.28$ ($k=1.6$) above threshold because computer limitations made it difficult to generate numerical wave functions of higher energy. Reducing the cutoff to $k=1.2$ changed the cross section in the region of interest by at most 5%, so this is an indication of the cutoff error. (5) The net error incurred in the evaluation of the sums over bound configurations, Eqs. (7) and (11), is felt to be negligible. (6) The ground state used for the computation of the dipole elements yields a high percentage of the correlation energy associated with the $2s$ electrons. Using a similar function, Weiss[8] was able to compute oscillator strengths using the length and velocity expressions which agreed to ~3%, so this function is not expected to be a significant source of error.

The computed ground-state energy of the $n=2$ shell is -1.0030. Combining this with the core energy taken from Ref. 9 yields a total ground-state energy of -14.6143 compared to Weiss's value of -14.6188.[8] Weiss used one additional configuration and his basis was different. The Hartree-Fock energy of beryllium is -14.5730;[7] thus the correlation energy for the present calculation is -0.0413, which is principally due to correlation among the $2s$ electrons. This may be compared with Kelly's perturbation theory result for the $2s$ correlation energy, which is -0.0439,[12] although the two numbers do not represent exactly the same quantity because the $1s$ function in the two cases differs. In the following, the Weiss value for the ground-state energy is used because the core is appropriate to the ground-state configuration. The excited states, on the other hand, are built upon a core appropriate for Be^{++}. Thus, in this manner, the differences in core energy between ground and excited states, although small, are largely allowed for. For the computation of the dipole elements, however, the function computed here is used.

As an aside, the basis set itself, without configuration interaction, is expected to give reasonable excitation energies for the $2snp$ configurations especially as n gets large because then correlation effects are less important, and the np orbitals are found in the Hartree-Fock field of $1s^22s$ Be^+. Table I compares some of these excitation energies with experiment and bears out the above remarks.

As a preliminary to obtaining the solution to Eq. (6), the matrix of the auto-ionizing configurations alone was diagonalized for both ^1P and ^3P symmetries. This calculation is analogous to earlier work on helium,[13] and the eigenvalues of the matrix should give the positions of the resonances except for the shift due to the continuum. The lowest five eigenvalues of the ^1P and ^3P matrices are given in Table II along with some experimental data and the recent close-coupling results of Moores,[14] which, of course, implicitly include the continuum shift. (Moores gives these energies with respect

TABLE I. Excitation energies of ^1P levels in beryllium. The experimental numbers were taken from Moore.[a]

	Present paper	Expt.
$2s2p$	0.2244	0.1939
$2s3p$	0.2857	0.2742
$2s4p$	0.3098	0.3063
$2s$ limit	0.3415	0.3426

[a] C. Moore, *Atomic Energy Levels*, Natl. Bur. Std. (U. S.), Circ. No. 467 (U. S. Government Printing Office, Washington, D. C., 1949).

[12] H. P. Kelly, Phys. Rev. **136**, B896 (1964).
[13] P. L. Altick and E. N. Moore, Phys. Rev. Letters **15**, 100 (1965).
[14] D. L. Moores, Proc. Phys. Soc. (London) **91**, 830 (1967).

to threshold so the experimental ionization potential was added in to give the numbers in the table.) The differences between the close-coupling and the discrete matrix energies then are a measure of the continuum shifts which are generally an order of magnitude larger than in helium because of the much stronger coupling in this case. Figure 1 compares coupling matrix elements in helium and beryllium. An especially large shift is apparent for the $2p3s$ level which is coupled most strongly to the continuum ($\Gamma \approx 0.4$ eV). (The reader may question why a larger shift is not observed also for the $2p3s\,{}^3P$ level. This level seems to have anomalous features such as a very narrow width; see Ref. 1 for a discussion.)

Because the widths of the $2pns$ levels are comparable to their separation, analysis of the levels as isolated resonances becomes tenuous and instead of assigning parameters to these resonances, the entire phase shift will be displayed. First, however, the $2pnd$ resonances will be parametrized since their widths are three orders of magnitude less than the $2pns$ and satisfy the isolated resonance approximation. Also, Moores's values for these widths are obtained by extrapolation rather than direct calculation. The resonance position E_r and width Γ are found in the usual manner, i.e., by fitting the phase shift δ to

$$\delta = \text{const} + \tan^{-1}[\tfrac{1}{2}\Gamma/(E_r - E)] \qquad (16)$$

in the vicinity of the resonance. The results for $2p3d$ and $2p4d$ are shown in Table III where they are compared with the extrapolated values of Moores who lists two sets of data, using different numbers of terms in the extrapolation. There is a large discrepancy for the $2p4d$ resonance wherein this calculation predicts a larger width than for $2p3d$. This occurs because—although both widths are small due to cancellations in the matrix elements—it happens that the cancellations are not so severe for $2p4d$ as for $2p3d$.

The phase shift, with respect to the $Z=1$ Coulomb wave, is shown as a function of energy in Fig. 2. Also shown is the close-coupling phase shift.[14] (In the figure the $2pnd$ resonances are not included. Their effect would be, of course, to raise the phase shift by π over a very narrow region.) The truncation in the $2p$ channel, i.e.,

TABLE II. ^1P and ^3P auto-ionizing levels in beryllium. The energy is given in eV above the ground state. The experimental data is from Moore.[a] The close-coupling results are from Ref. 14.

Designation	This paper ^1P	This paper ^3P	Close coupling ^1P	Close coupling ^3P	Expt. ^3P
$2p3s$	10.77	10.64	10.99	10.65	10.61
$2p3d$	11.86	11.81	11.93[b]	11.87	11.80
$2p4s$	12.07	12.03	12.13	12.05	
$2p4d$	12.47	12.44	12.52[b]	12.48	
$2p5s$	12.60	12.58	12.60	12.57	

[a] C. Moore, *Atomic Energy Levels*, Natl. Bur. Std. (U. S.), Circ. No. 467 (U. S. Government Printing Office, Washington, D. C., 1949).
[b] These levels were found by an extrapolation procedure.

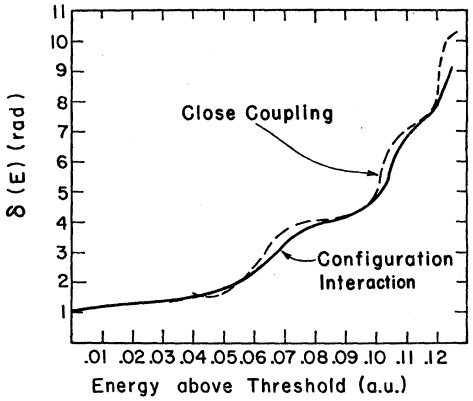

FIG. 2. The ^1P phase shift for electron scattering on Be^+ with respect to the $Z=1$ Coulomb wave. Shown also are the close-coupling results of Moores (Ref. 14). The effect of the $2pnd$ levels is omitted.

the inclusion of only eight configurations, causes the positions of the members of the auto-ionizing series to lie higher in energy and further apart than would be the case with no truncation. Cooper and Fano[15] have argued that in a Rydberg series of resonances, the ratio of width to the energy interval between members should be approximately constant. Thus the truncation also causes a broadening of the widths. Both of these effects are apparent in Fig. 2. Finally, note that the configuration-interaction phase shift just crosses the close-coupling phase shift at 0.05 a.u. whereas one expects from bound theorems that no crossing should occur. This is believed to be due to the different cores used in the two calculations which destroy the strict validity of the bound theorem in this case.

Before discussing the photo-ionization cross section, it is instructive to observe the high sensitivity to several approximations of the dipole matrix element at threshold. The crudest approximation is to compute

$$\langle \varphi_{2s} | r | \varphi_{\epsilon p} \rangle = \int r^3 dr\, \varphi_{2s}(r) \varphi_{\epsilon p}(r), \quad \epsilon = 0 \qquad (17)$$

using the basis functions. This is a poor procedure because the $2s$ function is not found in the potential appropriate for the ground state. It gives an element of -3.05 resulting in a cross section of 25.3 Mb. As an improvement, the Hartree-Fock $2s$ function appropriate for the ground state could be used in Eq. (17). This was essentially done by Kelly, yielding a cross section of ~ 0.9 Mb.[12] Yet a better approach is to compute

$$\langle \Psi_G | Z | \psi_{2s\epsilon p} \rangle, \quad \epsilon = 0 \qquad (18)$$

as the dipole element. Such a procedure is analogous to the calculations of Stewart and Wilkinson, and Stewart

[15] U. Fano and J. W. Cooper, Phys. Rev. **137**, A1364 (1965).

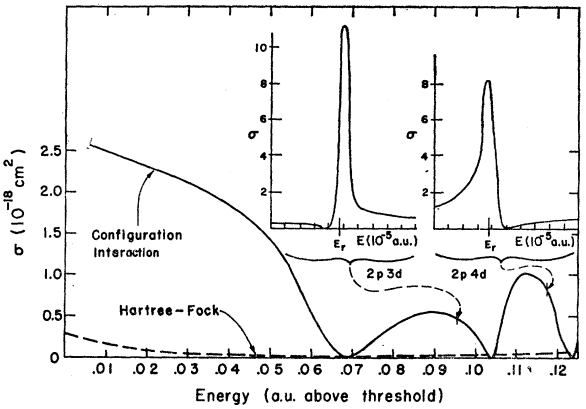

FIG. 3. The photo-ionization cross section of beryllium. The curve labeled "Hartree-Fock" was computed with the auto-ionizing lines omitted. The insets show the $2p3d$ and $2p4d$ line profiles whose location is designated by the arrows.

and Webb on helium.[16,17] The result is an element of 0.330 and a cross section of 0.295 Mb. Thus from the crudest to the best approximation the cross section changes by almost two orders of magnitude, and ground-state correlations alone lower it by a factor of 3.

The photo-ionization cross section is shown in Fig. 3. The $2pnd$ line profiles are shown as insets as these lines are much too narrow to appear on the main curve. They display the familiar Fano shape[18] and, treated as isolated resonances, have q values of $\sim+5.0$ and -3.1, respectively, for $2p3d$ and $2p4d$. The $2p3d$ profile is so narrow that only a crude fit could be obtained. The change in sign of the q values occurs because the dominant contribution to the background in either case is the closest $2pns$ resonance, but the dipole moment of $2p4s$ has the opposite sign from that of $2p5s$.

On the other hand, the $2pns$ levels are so broad compared to their separation that nothing resembling lines superimposed upon a background is apparent. The two "peaks" are due to the $2p4s$ and $2p5s$ levels, respectively, but where a large peak due to $2p3s$ is expected, the cross section is monotonically decreasing. This behavior can be traced to the combined effect of the first-order coupling of the $2p3s$ level and the second-order coupling of the bound configurations $2snp$. While it might be thought that such second-order effects should be small, the dipole moment of $2s2p$ is very large compared to $2p3s$ or $2s\epsilon p$, so a small coupling can result in a sizeable effect in the cross section. (Similar conclusions were arrived at in earlier work on beryllium.[10]) Thus near the threshold, the contribution of the bound configurations is dropping at a rate slightly greater than the rate of increase of the contribution of the $2p3s$. Eventually both contributions decrease with energy, resulting in a steep decline. The large increase in cross section or oscillator strength with respect to the contribution of the $2s$ continuum (which is plotted in Fig. 3 and is very small) is therefore not due solely to the auto-ionizing lines but near threshold is also due to transfer of oscillator strength from bound states to continuum states with the auto-ionizing levels acting as intermediaries.

It might be noted that the mechanism for transfer of oscillator strength in this way is included in Fano's treatment of auto-ionization.[18] Specifically, what Fano calls the modification of the auto-ionizing state by admixture of states of the continuum, Eq. (17) of his paper, contains an integral over the continuum which can be extended to include a sum over discrete terms of the Rydberg series. However, while Fano considered this modification to be a small effect, the sum makes a large, energy-dependent contribution to the cross section in beryllium. Therefore the line profile indices q, Eq. (20) of Ref. 18, are not even approximately constant over the width of a line, and the line shapes depart accordingly from those shown in Fig. 1 of Fano's paper.

Another interesting feature in the cross section is the fact that the $2p4s$ peak is lower than the $2p5s$. This comes about because of the sign change in the $2pns$ dipole moments mentioned above. The position of the sign change is such that the $2p4s$ moment is less than the $2p5s$.

Although there are at present no measurements of the photo-ionization cross section with which to compare, the type of agreement on the phase shift between this calculation and the recent close-coupling work indicates that the peaks in the cross section should be sharper, but no significant departure from the over-all shape is expected.

TABLE III. Positions (eV above the ground state) and widths (eV) of some $2pnd\ ^1P$ resonances in beryllium. Two different sets of extrapolated results (Γ_A and Γ_B) due to Moores (Ref. 14) are also included.

Designation	E_r	Γ	Γ_A	Γ_B
$2p3d$	11.91	5.94×10^{-5}	2.68×10^{-4}	3.95×10^{-5}
$2p4d$	12.49	1.93×10^{-4}	2.97×10^{-5}	1.72×10^{-5}

ACKNOWLEDGMENTS

This manuscript was completed while the author was at the University of Chicago. Support for this period from the Atomic Energy Commission (Report No. COO-1674-7) is gratefully acknowledged. Also, I would like to thank Dr. U. Fano for numerous clarifying discussions. Finally, I would like to thank D. L. Moores for providing numerical values of the phase shifts from which Fig. 2 was constructed.

[16] A. L. Stewart and W. J. Wilkinson, Proc. Phys. Soc. (London) **75**, 796 (1960).
[17] A. L. Stewart and T. G. Webb, Proc. Phys. Soc. (London) **82**, 532 (1963).
[18] U. Fano, Phys. Rev. **124**, 1866 (1961).